Classical dynamics of impulsively driven collisional energy transfer

G. Roberts
Department of Physics, University of Newcastle, Newcastle upon Tyne NE1 7RU, England
(Received 9 December 2000; published 17 September 2001)

This paper seeks to address the problem of collisional energy transfer between atoms or molecules arranged in connecting layers on a solid surface in response to impulsive photon impact. An analysis based on classical trajectories of the motions of a line of touching spheres subject to impact at one end, computed by Green's method, is adopted to describe the collisional behavior of atoms or molecules attached to a metal subsequent to electronic excitation by an ultrafast laser pulse. To highlight the essential dynamics, the characteristic line dissociation and rebound behavior of a series of connected spheres is investigated for different impact durations, amplitudes, and numbers of particles. The individual particle trajectories reveal the propagation of a disturbance along the line which results in fragmentation of the outermost particles from the remainder. In applying this scheme to energy transfer between molecules stacked on a low-temperature metal, a model of photon-induced, resonant electron scattering between displaced harmonic oscillators is invoked to estimate the magnitude of the impulsive force that acts on the atoms or molecules immediately adjacent to the solid surface. From the time-dependent line fragmentation velocities, kinetic energy distributions are calculated for photodesorption of benzene molecules from Pt{111} by a normally incident laser beam, and are compared with recent experimental measurements.

DOI: 10.1103/PhysRevA.64.042903 PACS number(s): 34.50.Dy, 31.70.Ks, 33.80.−b, 34.20.Gj

I. INTRODUCTION

The interaction of ultrashort light pulses with atoms and molecules at a solid surface is a subject of intense research activity on account of the range of physical phenomena that can be studied. These include: light absorption; electron and phonon scattering; atomic collisions; and desorption and ablation of atoms, molecules, and clusters. Experimental observations have recently been reported of the velocity distributions of intact benzene (Bz) molecules ejected from a platinum metal surface (Pt{111}) at 100 K by an ultrafast laser pulse [1]. The photon field penetrates the transparent molecular overlayer to interact with the conduction-band electrons of the metal. Measurements of the molecular desorption speed at a specific angle relative to the surface normal were made by recording the time-of-flight (TOF) of Bz trajectories in a mass spectrometer. From the results of experiments carried out using laser pulses of varying intensity and duration applied to different molecular thicknesses (from 2 to 20 layers), coupled with the use of deuterated benzene, it was suggested by the authors of Ref. [1] that molecular detachment from the solid was initiated by an impulsive force applied to the innermost molecule. The initial impact was postulated to originate from phonon-assisted, resonant electron scattering between molecular orbitals and the metallic conduction band, with subsequent energy transfer across the condensed molecular layers resulting in desorption of intact molecules at or near the molecule-vacuum interface. The present contribution seeks to study these phenomena from a classical dynamics perspective, adopting a simple theoretical model for the light-induced desorption force and impulsive energy transfer between molecules attached to the solid surface.

During the completion of this study, a paper was published by Hinch and Saint-Jean (hereinafter referred to as HSJ) [2], which addressed an analogous dynamical problem in the context of impacts on granular materials. These authors examined the Newtonian dynamics of a collection of touching particles subject to terminal impact, and formulated a theoretical model for the evolution of a spreading wave along a line of spheres connected by linear and 3/2-power-law contact forces, obtaining a similarity solution for its propagation with time. The temporal dependence of solitary waves along lines of particles has been studied numerically [3] and experimentally [4]. The dynamical behavior of lines of particles impacted at one end is identical to that of a series of ball bearings suspended from a thread between two stainless steel bars, an apparatus which constitutes an executive toy known (at least in the United Kingdom) by the epithet ''Newton's cradle.''

Differing from HSJ, in this paper we compute classical trajectories for a line of particles subject to impulsive forces of varying duration and amplitude, and connect these results to the question of laser desorption of molecules in multilayer configurations attached to a solid surface. In Sec. II we give the classical equations of motion for the problem and describe the numerical approach. The characteristic dynamical properties of such systems are examined in Sec. III, which briefly outlines the motions of a line of impulsively excited, connected spheres under different impact conditions. A model for laser desorption of layers of molecules from solid surfaces based on these results, together with numerical simulations of the kinetic energy distributions of Bz molecules photoejected from a Pt surface by a normally incident laser pulse, is described in Sec. IV. Shortcomings of the calculations in respect of its intended application are summarized in Sec. V and concluding remarks are given in Sec. VI.

II. CLASSICAL EQUATIONS OF MOTION

In this section we first give the classical equations of motion for a line of connected spheres and briefly outline

Green's method for calculating the trajectories of particles subject to an impulsive driving force. This constitutes the basis of the model of collisional energy transfer applied in Sec. IV. We also discuss the impact dynamics within an anharmonic potential, intended for atomic and molecular applications, and briefly describe numerical considerations relevant to carrying out these calculations.

A. Terminal impact on a line of connected spheres

We consider the one-dimensional motion of N particles each of mass m arranged in contact in a line. The classical equations of motion for such an arrangement have been given by HSJ [2], but for completeness are briefly re-stated here. Newton's equation of motion for any particle other than the two at the end of the line can be written

$$m\ddot{z}_n=[-F_{n-1}+F_n]+[F_n-F_{n+1}]$$
$$=k(z_{n-1}-z_n)_+-k(z_n-z_{n+1})_+, \tag{1}$$

where $z_n \equiv z_n(t)$ represents the displacement of the nth particle from its initial position in contact with its neighbors, $k=\omega_0^2 m$ and $n=2,\ldots,N-1$. When $n=1$ and $n=N$, the first and second terms, respectively on the right-hand side are omitted from the equation of motion. Equation (1) assumes a linear power law for the contact force between neighboring spheres, which is considered to be purely elastic and noncohesive. The value of either term in parentheses is taken to be zero if the enclosed expression is negative, thereby removing the possibility of tension between two particles; this is indicated by the subscript "+" appended to the closing parenthesis in the notation of HSJ [2]. To solve Eq. (1), initial conditions were chosen as

$$z_n(t=0)=0, \quad 1\leqslant n\leqslant N; \tag{2a}$$

$$\dot{z}_1(t=0)=\begin{cases} v_1, & n=1 \\ 0, & 2\leqslant n\leqslant N. \end{cases} \tag{2b}$$

Equations (2) correspond to the first particle impacting the remainder of a stationary line with a linear velocity $\dot{z}_1(t)=v_1$.

B. Impulsive impact of a line of connected particles

The transient behavior of a line of particles subject to an impulsive driving force at one end that acts for a time that is finite, but short in comparison with the natural oscillation period, may be obtained by Green's method [5]. The differential equation that describes the motion of the first (terminal) particle is

$$\ddot{z}_1+\omega_0^2(z_1-z_2)_+=\frac{F(t)}{m}, \tag{3}$$

for which the solution is

$$z_1(t)=\int_{-\infty}^{t} F(t')G(t,t')dt', \tag{4}$$

where $G(t,t')$ is the Green's function for the linear oscillator Eq. (3) [5] and $F(t)$ is the driving force. The impulse that is delivered to the first particle is subsequently transferred along the line of particles in contact. In the absence of damping, the equations of motion for all particles other than the first are, from Eqs. (1) and (3),

$$\ddot{z}_n-\omega_0^2(z_{n-1}-z_n)_+ +\omega_0^2(z_n-z_{n+1})_+=\frac{F'(t)}{m} 2\leqslant n\leqslant N-1 \tag{5a}$$

and

$$\ddot{z}_N+\omega_0^2(z_{N-1}-z_N)_+=\frac{F'(t)}{m} n=N, \tag{5b}$$

where $F'(t)=F(t)$ for perfect coupling of subsequent impacts along the line of fragmentation between oscillators; that is, it is assumed that there is no degradation of the terminal impact by energy dissipation into degrees of freedom orthogonal to the dissociation coordinate. For reasons of numerical convenience, we take $F(t)$ to be the Gaussian form,

$$F(t)=F_0\exp[-t^2/2\sigma_t^2],$$

characterized by a full width at half maximum (FWHM) $\tau_p=2\sqrt{\ln 2}\sigma_t$.

In respect of the intended application of Eqs. (3)–(5) to photon-initiated impulsive impact of atoms or molecules attached to a solid surface, a crucial concern is how the time dependence of $F(t)$ that acts on the terminal particle adjacent to the surface differs from the temporal envelope shape of the incident laser pulse. Except in the restricted example of direct dipole excitation of the innermost molecule by the laser pulse, $F(t)$ is modified by the dynamical reponse of the substrate to the photon field, and how that couples to atomic or molecular motions normal to the surface plane. In the case of Bz molecules transparent to the incoming radiation, the authors of Ref. [1(b)] put forward a model in which desorption driven by resonant electron scattering was mediated by phonon motions during the course of the laser pulse. To model the diverse multidimensional electronic and nuclear motions of the substrate and their influence on desorption modes demands a consideration of the time dependence of $F(t)$ beyond the scope of the present calculations, where the emphasis is on the dynamics associated with propagation of an impulse along a line of molecules (or atoms). For this reason, we examine how the line fragmentation patterns vary for different $F(t)$ characterized by values of τ_P spanning three orders of magnitude.

C. Impulsive impact of a line of connected anharmonic oscillators

In applying the approach of the previous section to collisions between atoms or molecules, it may be considered more sagacious to take account of the anharmonic character of interatomic and molecular forces. In Sec. IV we investigate the impact dynamics of a line of perfectly coupled Morse oscillators: this form was chosen because only one

further parameter, the dissociation energy D_e, is required in addition to the oscillator frequency to characterize the force field. In this case, Eq. (5a) becomes

$$\ddot{z}_n-\omega_0^2\left((z_{n-1}-z_n)_+-\frac{3}{2}\beta(z_{n-1}-z_n)_+^2\right)+\omega_0^2\left(z_n-z_{n+1})_+\right.$$
$$\left.-\frac{3}{2}\beta(z_n-z_{n+1})_+^2\right)=\frac{F'(t)}{m},\quad 2\leqslant n\leqslant N-1, \tag{6}$$

where the Taylor expansion of $\exp[-x]$ is curtailed at the third term and $\beta=\sqrt{m/2D_e}\omega_0$; Eq. (5b) is amended analogously. In these calculations no account is taken of Bz internal motions or how they couple to desorption along the surface normal. We also restrict our considerations to incident light fluences below that which causes ablation of solid microparticles and clusters into the gas phase; i.e., only line fragmentation to give intact, single molecules is investigated. Garrison and co-workers have developed a breathing sphere model for molecular dynamics (MD) simulations of laser desorption and ablation of molecular solids which takes into account internal molecular motions, translation of desorbed and ablated materials (atoms, molecules and clusters), and gas-phase collisional processes in the plume of ejected material formed immediately above the solid surface [7]. These MD simulations reveal that large molecular clusters comprise a substantial portion of the material photoejected from the surface of an organic solid above the ablation threshold by focused ultrafast laser radiation, and that collisional and dissociative processes in the plume which develops over a time scale of hundreds of picoseconds have a significant influence on the terminal velocities and angular distributions of gas-phase particles [7]. Such processes are likewise not included in the much simpler calculations of the line dissociation dynamics of intact molecules reported here.

D. Numerical solutions to classical equations of motion

Equations (3)–(6) were solved numerically by a fourth-order Runge-Kutta algorithm that included adaptive stepsize control [6]. As noted by HSJ, it was found that non-negligible, non-fourth-order errors were introduced into the solutions for large numbers of particles ($N\simeq 100$), arising from the discontinuous change in the derivative of the force between extension and compression of $z_n(t)$. Although the present study does not report on the dynamics for $N>20$, the selection of step size was controlled, as performed by HSJ [2], such that when particle $n+1$ lost contact with particle n during time step Δt_j, the increment in the time step was adjusted so that the separation occurred at the end of the time step, the correction being made to second-order accuracy from knowledge of z_n, $\dot{z}_n$, and $\ddot{z}_n$ at the beginning of the jth time step. Propagations were carried out for times at least ten times longer than $2\sigma_t$.

III. CLASSICAL DYNAMICS OF AN IMPULSIVELY DRIVEN LINE OF SPHERES

In prevenience to the molecular calculations presented in Sec. IV, we first discuss the impact dynamics of a line of touching spheres. The problem has been analyzed by HSJ [2]: it is included here for the conceptual insights it affords into the effect of changing the duration and amplitude of $F(t)$ and as a check of numerical procedures. In applying the methods of Sec. II to liftoff of atoms or molecules from a metal surface it is necessary to invoke approximations (described in Sec. IV) to estimate the magnitude of the initial driving force and the nature of the interatomic or intermolecular potentials. This section therefore describes the impulsive motions of a line of structureless spheres, which may be thought of in this context as atoms or molecules, so as to highlight the essential time dependences in the absence of such approximations. The results obtained here pertain to the study of impulse dynamics in different areas of physics: for instance, the motion of atoms in a long molecule or polymer; impacts on granular materials, as investigated by HSJ [2]; and to atoms and molecules stacked on a solid, as discussed in Sec. IV.

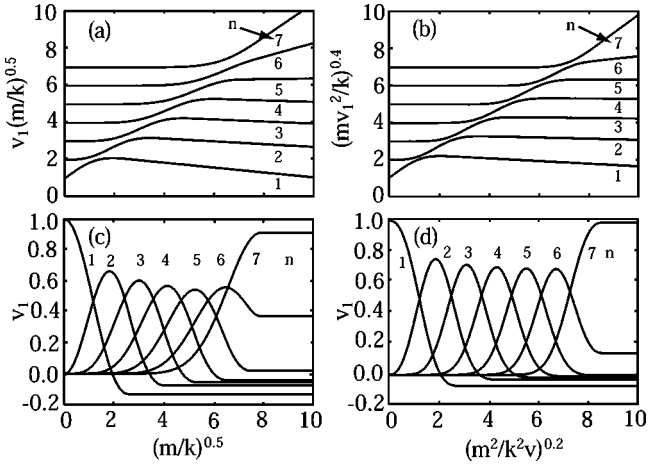

FIG. 1. Variation of displacements [(a) and (b)] and velocities [(c) and (d)] in time for seven touching particles in a line impacted at one end by particle 1 with unit velocity. Diagrams (a) and (c) show the dynamics for a linear contact force, diagrams (b) and (d) for 3/2-power law. For the linear contact force the time scale is given in increments of $(m/k)^{1/2}$ and the displacement scale is $v_1(m/k)^{1/2}$, where v_1 is the impacting velocity of particle 1. For the nonlinear contact force, the time scale is $(m^2/k^2v_1)^{1/5}$ and displacement scale is $(m^2v_1^4/k^2)^{1/5}$ [2]. In diagrams (a) and (b), the displacement of the nth particle is increased by n for clarity of presentation.

Figure 1 shows the trajectories and velocities of seven touching particles subject to impact at one end by particle 1 with a (dimensionless) velocity $v_1=1$, and is presented for direct comparison with Fig. 1 of the paper by HSJ [2]: Figs. 1(a) and (c) display the dynamics for a linear interparticle force, while Figs. 1(b) and (d) give analogous results for a force that depends on the separation of neighboring spheres to the power 3/2 [8]. For this number of particles and time scales $t\leqslant 10\sqrt{m/k}$ and $t\leqslant 10^5\sqrt{m^2/k^2v_1}$, both linear and nonlinear separation forces result in the same general patterns of temporal behavior, though differing in quantitative detail. The displacement versus time graphs have initial slopes that are zero for all particles except the first, and show that the displacement from pre-impact separation occurs sequentially for spheres further down the line. The graphs of velocity

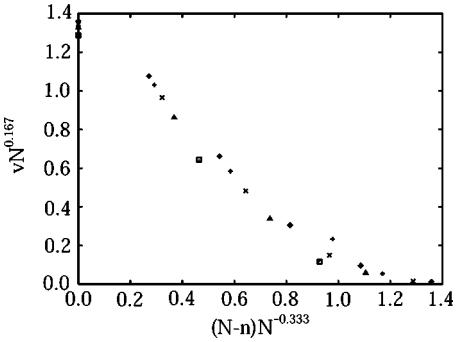

FIG. 2. Plot of the scaled final velocities $v_n N^{1/6}$ of n particles as a function of their position $(N-n)N^{-1/3}$ from the end of a line of N particles: triangles, $N=10$; diagonal crosses, $N=20$; rectangles, $N=30$; crosses, $N=40$; diamonds $N=50$.

versus time clearly reveal the temporal propagation of a disturbance along the line with a constant velocity of $v_n=1$, i.e., one particle per dimensionless unit of time. At times beyond $t \simeq 7\sqrt{m/k}$ [Figs. 1(a) and 1(c)] and $t \simeq 7.5\sqrt[5]{m^2/k^2 v_1}$ [Figs. 1(b) and (d)], contact between the particles ceases and their displacements vary linearly with time in accordance with Newton's first law. In this example, we see that particles 6 and 7 fly off the end of the line: the seventh with a velocity just below that of the impacting velocity of particle 1, while the sixth emerges at about $0.4v_1$ and $0.2v_1$ for the linear and 3/2-power contact forces, respectively. The remaining five particles rebound backwards after initial motion in the direction of the impacting particle. The analysis of HSJ leads to the expectation that when the impulse wave reaches the end of a line of discrete bodies, $O(N^{1/3})$ particles lose contact with the line with velocities $O(N^{-1/6})$ in the forward (impacting) direction [2]. These predictions are confirmed in Fig. 2, which displays the velocities at which particles are ejected from the line scaled by $N^{1/6}$ as a function of their position from the end of the line scaled by $N^{-1/3}$.

Figure 3 shows the displacements and velocities for seven touching particles subject to an impact of varying duration τ_p at a constant maximum amplitude $F_0=1$ applied to particle 1. In this calculation, $v_n(t=0)=0$ for all n, each particle is initially located at its equilibrium distance from its neighbor(s) and the interparticle force is linear in the separation. Several qualitative observations are apparent by inspection:

(i) For the impulsive driving force with $\tau_p=0.1\sqrt{m/k}$, the velocity of the first particle increases rapidly over a time scale $t \ll \sqrt{m/k}$ and then decreases. For particles 2–6, the slower increase and decrease in v_n images the Gaussian temporal envelope of the applied impulse. For $F_0=1$, the sixth and seventh particles are ejected from the line. [Particle 6 returns to the line over a time scale approximately 100 times longer than shown in Figs. 3(a) and (d).]

(ii) When $\tau_p \simeq \sqrt{m/k}$, the increase in velocity of the first particle is slower than for the shorter duration pulse, in line with the slower turn-on of $F(t)$, and the maximum velocity attained by the particles is greater, resulting in a larger displacement at a given time for $t \geqslant 2.5\sqrt{m/k}$. In this case, particles 6 and 7 initially fragment from the line, though the sixth particle eventually rebounds to rejoin the remainder.

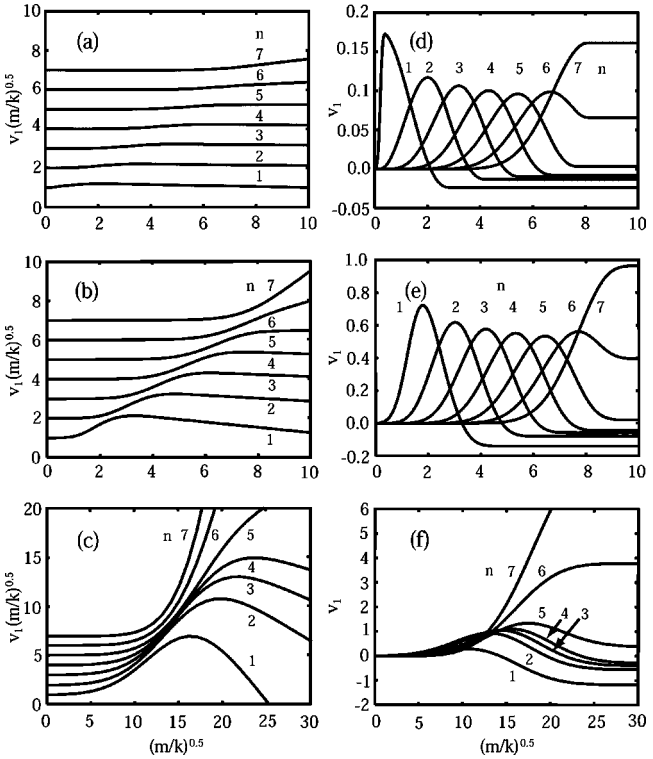

FIG. 3. Time-dependent displacements [(a)–(c)] and velocities [(d)–(f)] for seven particles in a line subject to a Gaussian temporal impulse of varying FWHM τ_p and constant maximum amplitude $F_0=1$ applied to particle 1: $\tau_p/(m/k)^{1/2}=0.1$ [(a) and (d)]; $\tau_p/(m/k)^{1/2}=1.0$ [(b) and (e)]; $\tau_p/(m/k)^{1/2}=10.0$ [(c) and (f)]. Displacement, velocity, and time scales are the same as in Figs. 1(a) and (c) and the displacement of the nth particle is increased by n.

(iii) The longest-lasting impact, with $\tau_p=10\sqrt{m/k}$, results in dissociation of the last two particles over a longer time scale with substantially increased forward velocities. [The fifth particle returns to the line over a time scale 10^3–10^4 times longer than shown in Figs. 3(c) and (f).]

(iv) The overall effect of increasing impact duration is to delay the onset of line oscillation and fragmentation, and to initiate a more violent disturbance.

Similar behavior pertains when the amplitude of the driving force is increased for a given pulse duration, displayed in Fig. 4 for $\tau_p=0.1\sqrt{m/k}$. For $F_0=5$, the line motions resemble the dynamics shown in Figs. 3(b) and (e), with forward ejection of particles 6 and 7 and eventual rebound of the remainder. The effect of increasing F_0 to 10 and 100 is an increase in line fragmentation: the separation velocity of the last two particles increases linearly with F_0, though fragmentation begins at the same time, and the difference between terminal forward velocities of particles 6 and 7 is independent of F_0. Forces with still larger amplitudes (not shown in Fig. 4) bring about ejection of particles further removed from the end of the line in the forward direction, albeit at reduced velocities.

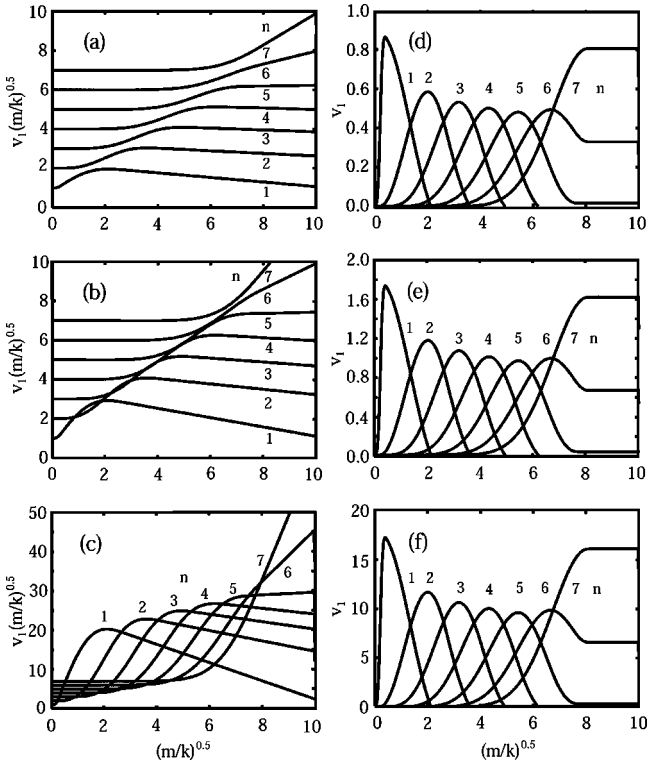

FIG. 4. Time-dependent displacements [(a)–(c)] and velocities [(d)–(f)] for seven particles in a line subject to a Gaussian temporal impulse of varying maximum amplitude F_0 and constant FWHM $\tau_p=0.1(m/k)^{1/2}$ applied to particle 1: $F_0=5$ [(a) and (d)]; $F_0=10$ [(b) and (e)]; $F_0=100$ [(c) and (f)]. Displacement, velocity, and time scales are the same as in Figs. 1(a) and 1(c) and the displacement of the nth particle is increased by n.

The change in dynamical behavior that occurs when the number of particles is altered is illustrated in Fig. 5, from which it is clear that the impulse generated by the intial impact always propagates along the line until one or more terminal particles dissociate. Figure 6 shows what happens when the zero tension condition otherwise applied in all calculations is relaxed: the particles remain in contact and propagate as a group to larger displacements, the individual trajectories displaying characteristic oscillations due to intracluster motions.

IV. IMPULSIVE ELECTRON SCATTERING AS AN INITIATOR OF MOLECULAR EXCITATION AND ENERGY TRANSFER

In this section, the model of Sec. II is applied to the situation of impulsive desorption of molecules from a metal surface, the process being initiated by an ultrafast laser pulse over a time scale shorter than, or at most comparable to, the intermolecular oscillation period. As has been stressed elsewhere [9], many (if not most) dynamical processes at metal surfaces triggered by ultrafast laser irradiation are initiated by excitation of valence electrons of the metal, which resonantly scatter between it and the attached atoms or molecules on a time scale of typically tens of femtoseconds [10–12]. As a result, theories of hot electron-stimulated photoinitiated dynamics at surfaces have been formulated which aim to calculate experimentally observable attributes of the desorption (such as gas-phase yields and final quantum-state distributions) from an analysis of the nonequilibrium electronic motions. In the regime where the desorption yield is linearly proportional to the fluence of the incident light, models which invoke a single inelastic scattering event between the molecule and a ballistic hot electron have been developed [9,13,14]; desorption of intact molecules that varies nonlin-

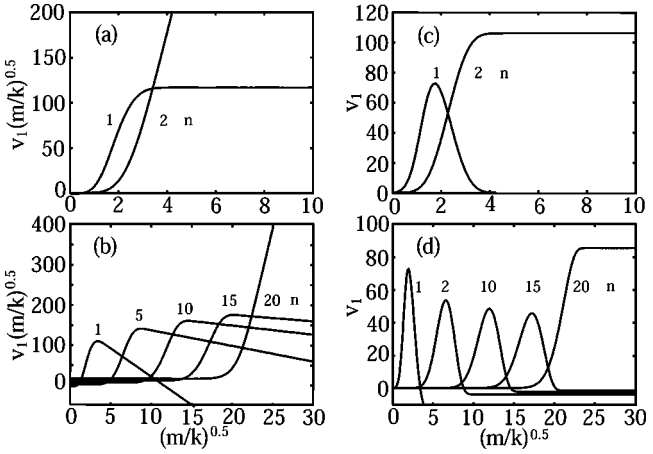

FIG. 5. Time-dependent displacements [(a) and (b)] and velocities [(c) and (d)] for differing numbers of particles in a line subject to a Gaussian temporal impulse with $\tau_p=1.0(m/k)^{1/2}$ and $F_0=100$ applied to particle 1: $N=2$ [(a) and (c)]; and $N=20$ [(b) and (d)]. The interparticle force is taken to be linear in the separation. The displacement, velocity, and time scales are the same as in Figs. 1(a) and 1(c), and the displacement of the nth particle is increased by n.

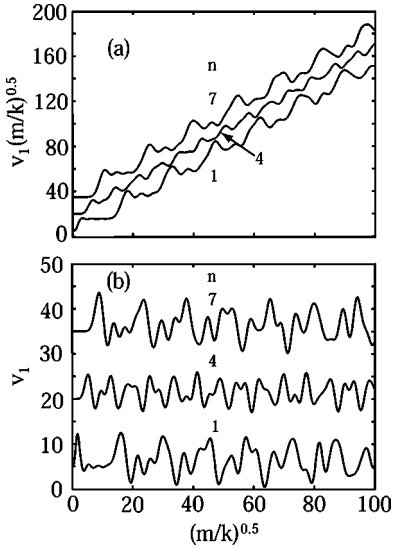

FIG. 6. Trajectories (a) and velocities (b) for seven particles in a line that can remain in tension subject to an initial Gaussian driving force with $\tau_p=1.0(m/k)^{1/2}$ and $F_0=10.0$. The interparticle force is linear in the separation and the displacement, velocity, and time scales are the same as in Figs. 1(a) and 1(c). Displacements and velocities are increased by $5n$ for clarity, for which reason also, results for $n=1$, 4, and 7 only are displayed.

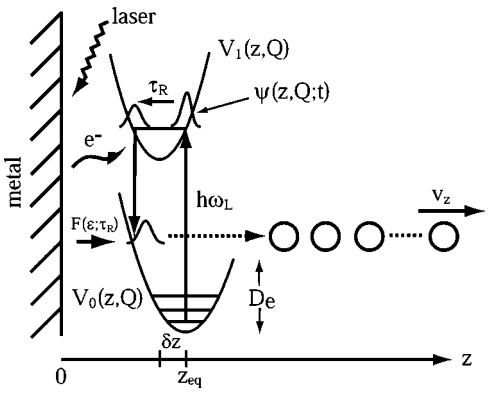

FIG. 7. A mixed quantal/classical cartoon of electron-molecule scattering at a metal surface, induced by an ultrafast laser pulse of photon energy $\hbar\omega_L$, which brings about line fragmentation of atoms or molecules lined up normal to the metal surface indicated left by the hatched region. The transient, negative-ion wave-packet state $\psi(z,Q;t)$ generated by resonant electron scattering transits over the harmonic potential $V_1(z;Q)$ for a period τ_R. After this time, $\psi(z,Q;\tau_R)$ is coherently deposited as a superposition of bound and continuum levels supported by the ground electronic state, here represented by a harmonic oscillator potential $V_0(z;Q)$ truncated at the dissociation energy D_e on the large z side. Liftoff of intact atoms/molecules (represented by classical spheres) subject to terminal impact at the metal surface proceeds along the z coordinate, the outermost sphere departing with a velocity v_z along the surface normal. (Q denotes all other nuclear degrees of freedom.) Adapted from Fig. 3 of Ref. [26(b)].

early with laser fluence has been treated in terms of multiple electronic transitions between adsorbate neutral and ionic states [9(b),14,15], by multiple scattering of thermionic hot electron fluxes emanating from within the metal [16] and by stochastic processes driven by electronic friction [17]. These notions are supported by a wealth of experimental evidence on shape resonance-enhanced desorption of molecules such as NO, O_2, and CO from Pd, Cu, and Pt surfaces by femtosecond laser pulses [18,19], though the multiplicity of scattering at high incident fluences would appear to remain a question for further investigations [16]. The basic ideas of the model based on a single ballistic electron scattering event, as applied to photodesorption of Bz from Pt [1], are encapsulated in Fig. 7. Referring to the figure, a brief qualitative description of resonant desorption in the style of Gadzuk [9] proceeds along the following lines. First, the incident radiation (of photon energy $\hbar\omega_L$) creates a high, nonequilibrium distribution of hot conduction-band electrons above the Fermi level by photon absorption within the metal. This results in a flux of electrons from the metal which are temporarily captured by adsorbed molecules adjacent to the surface, thereby generating a negative-ion state on the potential $V_1(z;Q)$. The postulate of Ref. [1(b)] is that this process is pre-empted by, and assisted by, preheating of the (Bz)-metal complex by excitation of low-frequency vibrational modes of the molecule. The residence time τ_R of negatively charged adsorbate-induced resonances has been variously determined to be between 0.8 and 250 fs for different adsorbate-metal combinations by two-photon photoelectron emission (2PPE) spectroscopy [10,11]. The lifetimes of image-potential states, determined by the same technique, are found to range from tens of femtoseconds to greater than 1.5 ps [20,21]. At the end of the period τ_R, the hot electrons relax into unoccupied conduction band states of the metal [10–12,22,23], leaving the attached molecule distributed among continuum levels supported by the neutral ground-state potential $V_0(z;Q)$ above the threshold for desorption, as well as vibrationally excited bound states. Since this superposition state contains continuum eigensolutions to the Hamiltonian associated with $V_0(z;Q)$, it leads to liftoff of the intact molecule from the surface. Gadzuk [9(a),24] has stressed the importance of the magnitude of τ_R, which is determined by the derivative of the phase shift of the dominating partial wave that characterizes the shape resonance with respect to energy [25], compared the relevant dynamical time scale (here, the vibrational period along the desorption coordinate), in controlling molecular nuclear dynamics on the surface.

In the present context, our interest is to estimate the amplitude of the time-varying force $F(\epsilon;t)$ that acts on the localized wave-packet state resonantly dumped on $V_0(z;Q)$ at a center energy ϵ by correlated hot-electron scattering and rescattering, since this is required for input into Eq. (3). To determine the impulsive kick imparted to a molecule adjacent to the surface, we consider a representation of the neutral and ionic electronic states by displaced, identical harmonic oscillator (HO) potentials [26], illustrated as $V_0(z;Q)$ and $V_1(z;Q)$ in Fig. 7. (Here, z denotes the desorption coordinate and Q represents all other nuclear degrees of freedom.) In reality, $V_1(z;Q)$ is likely to be more tightly contracted due to enhanced electrostatic [9(a),24,26(a),27] and electrodynamic (''chemical'') [28] attractive forces. It is assumed that the excited ionic potential is centered at shorter z as a result of electrostatic attraction between the residual positive charge of the metal and the electron trapped in the shape resonance. Models based on displaced harmonic or anharmonic oscillators have been applied extensively to problems associated with resonant electron-stimulated dissociation of molecules from metals [9,13,26]. Within the framework of fast sequential desorption events outlined above, the force $F(\epsilon;\tau_R)$ acting upon the superposition state $\psi(z,Q;t)$ returned to $V_0(z;Q)$ with a center energy ϵ at time $t=\tau_R$ may be conveniently expressed as a sum of two parts,

$$F(\epsilon;\tau_R)=F_1(\epsilon;\tau_R)+F_2(\epsilon;\tau_R). \tag{7a}$$

The first component F_1 derives from the momentum gained by the evolution of $\psi(z,Q;t)$ over $V_1(z;Q)$ for a period τ_R. When $V_0(z;Q)$ and $V_1(z;Q)$ are simple HO potentials with the same oscillation frequency ω_0, this contribution may be written

$$F_1(\epsilon;\tau_R)=-m\omega_0^2\delta z\cos(\omega_0\tau_R), \tag{7b}$$

where δz is the displacement of $V_1(z;Q)$ along the desorption coordinate relative to $V_0(z;Q)$ as defined in Fig. 7. Equation (7b) is a classical result based on Ehrenfest's principle, in that it assumes that the spatial extent of the wave packet $\psi(z,Q;t)$ deposited on $V_0(z;Q)$ remains very small in comparsion to the dimensions of the potential energy

curves $V_1(z;Q)$ and $V_0(z;Q)$ along the z coordinate; for molecules attached to metals, Ehrenfest's principle is likely violated within a half period of the round-trip time of $\psi(z,Q;t)$ on $V_1(z;Q)$ by rapid phase-changing processes such as electron-hole, electron-phonon, and electron-electron scattering [22,23]. The second component of the force is due simply to the ground-state potential gradient at $z(\tau_R)$, i.e.,

$$F_2(\epsilon;\tau_R) = -\left.\frac{\partial V_0(z;Q)}{\partial z}\right|_{z=z(\tau_R)} = -m\omega_0^2[z(\tau_R)-z_{eq}], \tag{7c}$$

where z_{eq} is the equilibrium distance between the electronic minimum of $V_0(z;Q)$ and the metal surface.

Within the terms of this model, calculation of $F(\epsilon;\tau_R)$ necessitates knowledge of $V_0(z;Q)$, $V_1(z;Q)$, and τ_R. For Bz attached to Pt{111}, the following spectroscopic information is available: the oscillation frequency $\omega_0 = 360\ \mathrm{cm}^{-1}$ [29], assumed to be independent of layer thickness in the absence of quantitative information about how it may change; and the dissociation energies $D_e = 0.54$, 0.48, and 0.50 eV for layers $n=2$, 3, and 4, respectively [30]. These values are consistent with known information on the structures of Bz layers adsorbed on Pt{111} and Ru{001}, which have been the subject of a series of studies by electron energy-loss and other surface spectroscopies over 28 years [30–33]. These indicate that whereas the innermost chemisorbed layer lies parallel to the surface for both metals [30,32], in the second (i.e., first physisorbed) layer [α_1] the hexagonal rings are oriented at a high average tilt angle relative to the crystal surface face when higher layers are present, at least in the case of Bz adsorbed on Ru{001} [33]. For the same metal, the third [α_3] and other intermediate layers that constitute the bulk crystalline phase also adopt a configuration in which molecules are more or less upright, with a high average tilt; molecules in the topmost metastable layer [α_2'] are randomly oriented [33]. This simplified picture neglects the formation of two- and three-dimensional islands, which are known to occur for Bz adsorbed on Ru{001} [33]. In the absence of prior knowledge on the binding of the innermost ($n=1$) layer to the metal, it is assumed here that the desorption energy D_e(Pt-Bz) of the chemisorbed layer is 1.08 eV [34], i.e., twice the binding energy of the first physisorbed layer, which at least has the merit of qualitative agreement in trend with a measured binding energy for Bz on Cu{111} and an estimate for Bz on Ag{111} [35]. For $n>4$, D_e for $n=4$ is assumed.

According to the authors of Ref. [1(b)], desorption of Bz multilayers by 100 fs laser pulses begins at the leading edge of the temporal intensity envelope by a phonon-induced heating of a low-frequency Pt-Bz mode sufficient to populate the $q=10$ vibrational level of $V_0(z;Q)$, followed during the remainder of the pulse by single-photon excitation at $\hbar\omega_L = 1.55$ eV to a transitory negative-ion resonance state (Fig. 7). Desorption of the outermost molecules is postulated to result from subsequent energy transfer across the Bz layers. To estimate $F(\epsilon;\tau_R)$ the following procedure was therefore adopted, working within the framework of the displaced HO model illustrated in Fig. 7; the approach follows that espoused by Gadzuk [9] and applied by him [16,24,26] and others [13,14] to treat resonant molecular desoprtion phenomena. Using the quantum theory of forced oscillators, Korsch *et al.* have shown that a ground-state HO subject to an arbitrary, time-dependent force attains a Poisson distribution,

$$P_{q\leftarrow 0}(t) = \exp[-\alpha(t)]\frac{\alpha^q(t)}{q!},$$

of final states $|q\rangle$ as $t\rightarrow\infty$ [36]. For displaced HO's of the same frequency, the dynamic Poisson parameter $\alpha(t)$ is simply

$$\alpha(t) = 2\alpha_0(1-\cos\omega_0 t),$$

where α_0 may be identified as $\alpha_0 \equiv m\omega_0\delta z^2/2\hbar$ [9,26]. If it is assumed that the negative ion state decays exponentially at a rate $\Gamma = 2\pi/\tau_R$ [9(a),24,26] then $P_{q\leftarrow 0}(t)$ must be averaged over all times weighted by an existence probability, i.e.,

$$\langle P_{q\leftarrow 0}(\tau_R)\rangle = \int_0^\infty \frac{1}{\tau_R} P_{q\leftarrow 0}(t)\exp[-t/\tau_R]dt.$$

Unfortunately, little information appears to be known about the spectroscopy and lifetime of the excited state of Bz attached to Pt{111}. For up to five layers of Bz attached to Ag{111}, Harris and co-workers have recently determined resonance lifetimes of between $\tau_R = 20$ and 50 fs for the $n=1$ image-potential states from 2PPE measurements [21(a)], while Wolf and co-workers have previously reported $\tau_R = 40$ and 20 fs for the two lowest image-potential states of mono- and bilayers of Bz adsorbed on Cu{111} [21(b)]. These states were, however, determined to lie at energies greater than 3 eV above the neutral ground state in both cases. Without further quantitative information to hand, we assume here a value of $\tau_R = 30$ fs for a state populated by 1.55 eV photons. Maximizing $P_{q\leftarrow 0}(t)$ for the eleventh vibrational level of $V_0(z;Q)$ in accordance with the suggestion of Ref. [1(b)] enables an estimate of δz to be made for input into Eq. (7b), while the separation $z(\tau_R)-z_{eq,0}$ at the energy $\epsilon_{q=10} = 0.47$ eV of the $q=10$ vibrational level enables $F_2(\epsilon;\tau_R)$ to be determined from Eq. (7c). [$\langle P_{q\leftarrow 0}(\tau_R)\rangle$ always displays a maximum at $q=0$ assuming an exponential decay rate with $\tau_R \leqslant 150$ fs.] This procedure yields an initial force of magnitude $|F(\epsilon;\tau_R)| \simeq 20$ nN acting on the innermost Bz molecule in the direction of increasing z [implied by the minus signs in Eqs. (7b) and (7c)] as a result of resonant electron scattering and rescattering to and from $V_1(z;Q)$. Because of the approximate nature of this estimate, we test for the sensitivity of computed kinetic energy distributions to the value of $F(\epsilon;\tau_R)$ used as input to Eq. (3) (see below). The amplitude $F_0 = F(\epsilon;\tau_R)$ estimated from Eq. (7a) is based solely from electron dynamics over displaced harmonic oscillator potentials. Not knowing the temporal shape of the electron flux created by the laser pulse, the coupling of electron and lattice modes [37], and how their time-varying distribution functions together disrupt the forces between the

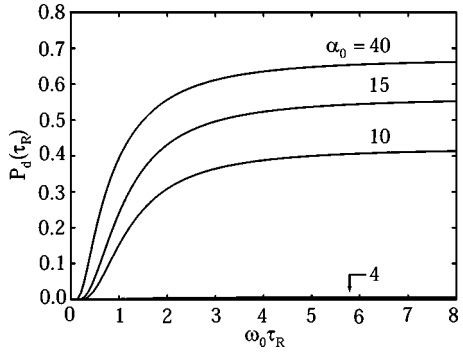

FIG. 8. Variation of the desorption probability $P_D(\tau_R)$ calculated according to Eq. (8), plotted as a function of $\omega_0\tau_R$ for different values of $\alpha_0=40$, 22.5, 10, and 4 treated as a parametric variable.

metal and the molecules at the surface, we investigate here impacts $F(t)$ with durations (FWHM) spanning three orders of magnitude that encompass the range of laser pulse durations used in the experiments of Ref. [1]. As discussed in Sec. II B, it is assumed that coupling of collisional energy between layers is identical for each neighboring pair and that there is no damping along the separation coordinate due to mixing of the desorptive motion with other vibrational degrees of freedom available to the system.

As an aside, knowledge of $P_{q\leftarrow 0}(t)$ enables a desorption probability $P_D(\tau_R)$ to be calculated from [9,24,26]

$$P_D(\tau_R)=\sum_{q=q_d}^{\infty}\langle P_{q\leftarrow 0}(\tau_R)\rangle, \tag{8}$$

where q_d is the lowest value of q for which

$$(q+0.5)\hbar\omega_0 > D_e\,.$$

Figure 8 shows the dependence of $P_D(\tau_R)$ on the resonance time τ_R for different values of α_0 corresponding to values of F_1 between 18.5 and 5.8 nN [$F(\epsilon;\tau_R)$ between 20.0 and 7.3 nN]: for $F(\epsilon;\tau_R)=20.0$ nN, giving a maximum at $q=10$ for $P_{q\leftarrow 0}(t)$, we see that $P_D(\tau_R)$ attains an asymptotic value of 0.66 after $\omega_0\tau_R\simeq 7$. Further discussion of the variation of $P_D(\tau_R)$ with τ_R may be found in Refs. [9] and [24(a)].

Figure 9 shows the time-dependent displacements and velocities for $N=2$, 10, and 20 benzene molecules attached to Pt, calculated from Eq. (6) on the basis of the model described above, subject to an initial impact with $F_0=20$ nN and $\tau_p=100$ fs. For these impulse parameters, the line-dissociation behavior is qualitatively similar to that shown in Figs. 4(b) and 4(f) and Fig. 5 for impacted spheres arranged in a line of varying length. When $N=2$, the nonimpacted particle flies off with a velocity that is essentially the same in magnitude as that of the impacting particle, which itself rebounds in the backwards direction. For $N=10$, the three endmost particles fragment from the rest of the line while the remainder rebound, albeit at different speeds, as found earlier [Figs. 4(c) and 4(f)] for a linear contact force between spheres. Similar behavior pertains for $N=20$, when four particles dissociate from the line. The fragmentation velocities

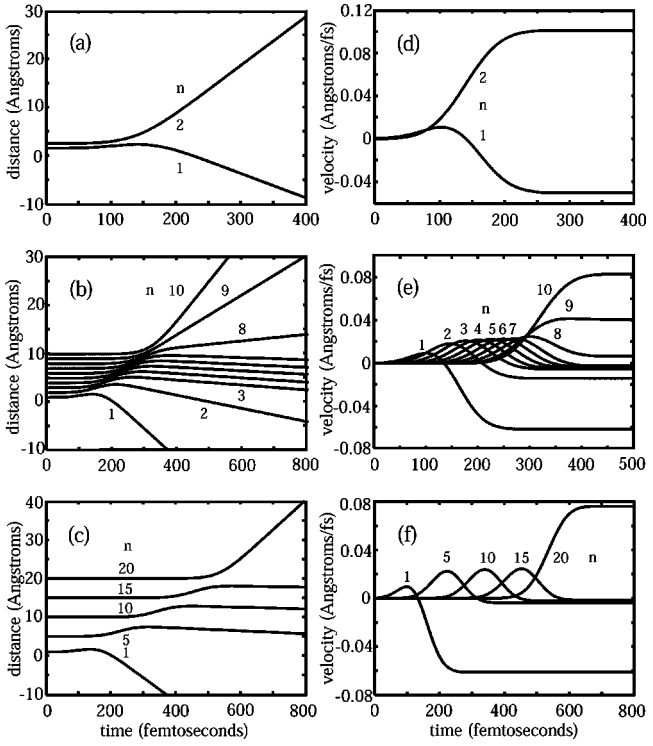

FIG. 9. Time-dependent displacements [(a)–(c)] and velocities [(d)–(f)] of $N=2$, 10, and 20 touching benzene molecules subject to a Gaussian temporal impulse with FWHM $\tau_p=100$ fs and maximum amplitude $F_0=20$ nN applied to the innermost molecule ($n=1$): $N=2$ [(a) and (d)]; $N=10$ [(b) and (e)]; $N=20$ [(c) and (f)].

v_N of the outermost particles in the forward direction decrease by $\simeq 25\%$ from $N=2$ to 20 for this combination of τ_p and F_0. In contrast, the velocity v_{N-1} of the penultimate particles increases by $\simeq 20\%$ from $N=10$ to 20, with the ratio v_{N-1}/v_N increasing from 0.49 at $N=10$ to 0.65 at $N=20$.

For a given number of particles, the variation of molecular displacements as a function of the duration of $F(t)$ at constant F_0 is presented in Fig. 10, while the behavior as F_0 is changed at a constant impulse width of $\tau_p=100$ fs is given in Fig. 11; in both cases, results for $N=7$ and $N=20$ are given as examples. The variation of molecular velocities with time is not displayed, but is qualitatively analogous to that given in Figs. 3(d)–3(f) and Figs. 4(d)–4(f). Figures 10 and 11 reveal that desorption of the two particles furthest removed from the impact source with velocities close to the initial impact remains an intact feature of the dynamics for different τ_p and F_0 (and N, for $N\geqslant 4$). For particular combinations of τ_p and F_0 when N is sufficiently large ($N\geqslant 5$), it is possible to induce additional line fragmentation, whereby an increasing number of particles originally located in the central portion of the line loses contact with the remainder.

Figures 9–11 display results which can be connected, at least in a qualitative fashion, to the experimental TOF spectra for dissociation of Bz from Pt obtained by Arnolds *et al.* [1], specifically with the TOF data recorded as a function of

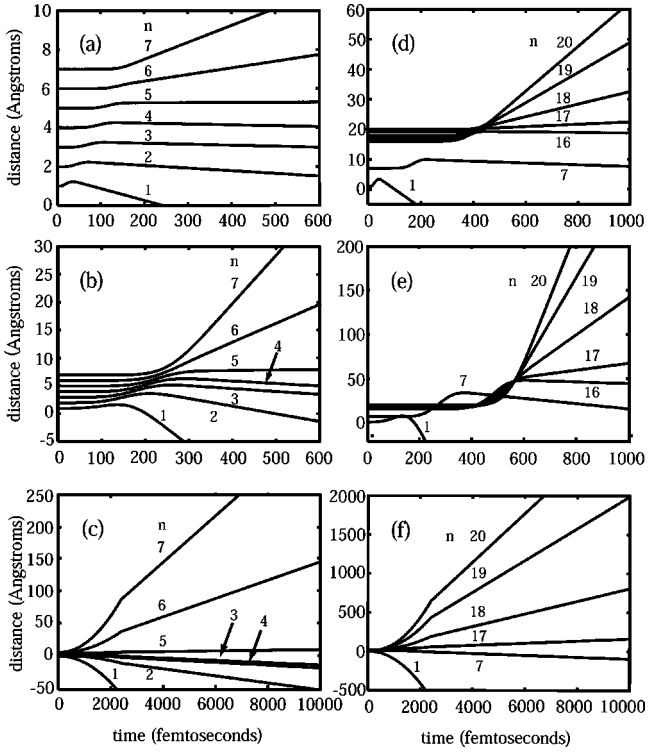

FIG. 10. Time-dependent displacements for $N=7$ [(a)–(c)] and $N=20$ [(d)–(f)] touching benzene molecules subject to Gaussian temporal impulses of fixed maximum amplitudes $F_0=20$ nN ($N=7$) and $F_0=200$ nN ($N=20$) and varying width τ_p applied to the innermost molecule: $\tau_p=10$ fs [(a) and (d)]; $\tau_p=100$ fs [(b) and (e)]; $\tau_p=1000$ fs [(c) and (f)].

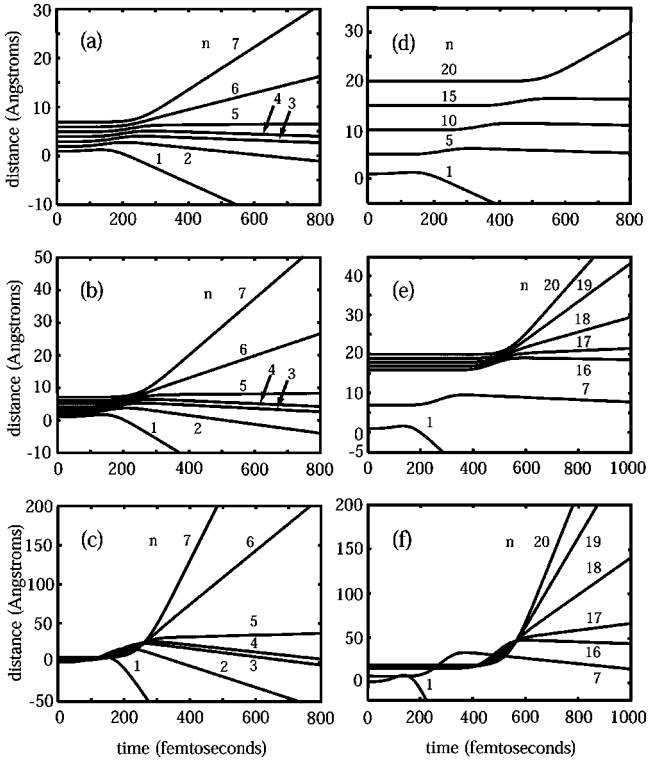

FIG. 11. Time-dependent displacements for $N=7$ [(a)–(c)] and $N=20$ [(d)–(f)] touching benzene molecules subject to Gaussian temporal impulses of fixed duration $\tau_p=100$ fs and varying maximum amplitude F_0 applied to the innermost molecule: $F_0=10$ nN [(a) and (d)]; $F_0=20$ nN [(b) and (e)]; $F_0=200$ nN [(c) and (f)].

Bz coverage (Fig. 1 of Ref. [1(a)] and Fig. 2 of Ref. [1(b)]), pulse width (Fig. 4 of Ref. [1(b)]) and laser fluence (Fig. 5 of Ref. [1(b)]). Removal of the outermost particle with highest velocities may be associated with the appearance of a ''high-energy'' peak of desorbed molecules in the experimental TOF spectra. The departure velocities of the secondary fragmentation process are somewhat lower than those for loss of the outermost particles, and may be connected with the slower, ''thermal'' benzene desorption feature noted in the laboratory. For large driving forces (e.g., $F_0=200$ nN) applied for long enough ($\tau_p \geqslant 100$ fs) and long lines ($N \simeq 20$), a third low-velocity fragmentation of the line occurs; and this may be associated with the slow, so-called ''subthermal'' desorption route monitored experimentally under conditions of photodesorption of thick Bz layers by 100 fs laser pulses [1]. Within this scenario, it is not necessary to invoke either cluster formation nor long surface residence times to account for subthermal line dissociation [1].

The results presented so far have not taken into account the spatial dependence of the intensity of the incident laser beam, i.e., we have assumed irradiation of a ''tube'' of benzene molecules stacked perfectly one upon the other while, somewhat in contradiction, recognizing a difference in stacking configuration in different layers to define a z-dependent oscillator frequency through the agency of a local dissociation energy. We now introduce the x and y spatial profile of the incident laser pulse to calculate distributions of desorption velocity which can be compared directly with experiment. To achieve this, several simplifying assumptions are made. The first is that it is assumed that the laser beam, propagating through the transparent molecular overlayers, is incident on the metal normal to its surface with a spatial intensity dependence given by the two-dimensional Gaussian form,

$$I(x,y)=I_0 \exp[-(x^2+y^2)/4\sigma_s^2], \tag{9}$$

where $\sigma_s=39$ μm is chosen to correspond to a disc of 270 μm in diameter at $I/I_0=0.025$ illumination in an attempt to mimic experimental conditions [1]. Here, I_0 may be regarded as an arbitrary (time-dependent) normalizing parameter; in the laboratory it corresponds to the use of a half wave plate and polarizing optic to generate different laser intensities. The spatial intensity distribution within the illuminated area is discretized in units of the dimensions of irradiated Bz molecules, taken to be elongated hexagons of length 11.08 Å and width 9.60 Å [31(b)]. We take no account of the detailed packing arrangement of Bz molecules attached to Pt in the x and y dimensions, though information for multilayer coverages on different metals is increasingly available from infrared spectroscopy [30,33] electron diffraction and Auger spectroscopy [31], and electron energy-loss measurements [32]. Nor do we discriminate between changes in intermolecular structure as a function of layer thickness

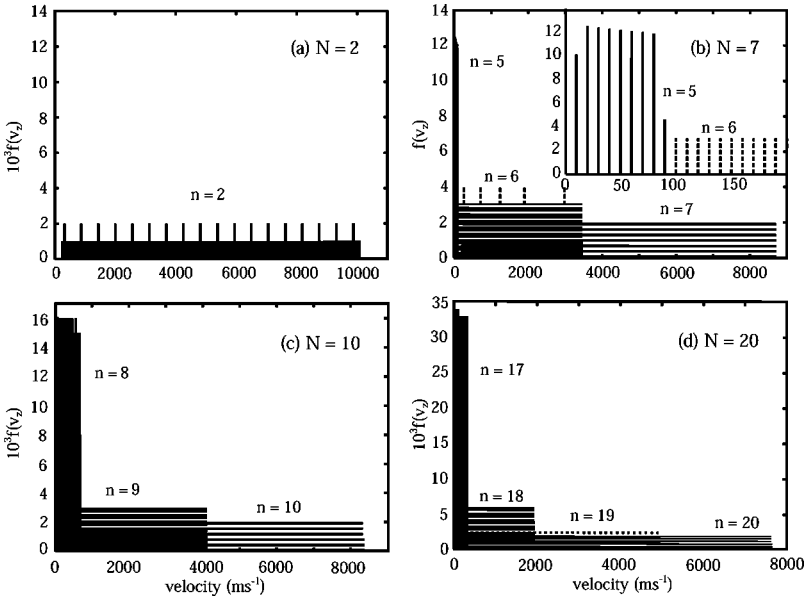

FIG. 12. Bar charts showing the fraction $f(v_z)$ of molecules with desorption velocities v_z normal to the surface plotted as a function of v_z for $N=2$ (a), 7 (b), 10 (c), and 20 (d) molecular layers subject to terminal impact on the innermost layer by a Gaussian force of FWHM $\tau_P = 100$ fs and maximum amplitude $F_0=20$ nN. Panels (a), (c), and (d) display $10^3 f(v_z)$ for all n; panel (b) and its inset display $10^2 f(v_z)$ $(n=5)$ and $10^3 f(v_z)$ $(n=6$ and 7). The bin size dv_z is 10 ms^{-1} for all panels.

[30,33]. It is further assumed, with no formal justification, that F_0 is directly proportional to the laser intensity $I_0(t)$ through the action of the **E** vector of the light on the metal electron cloud; i.e., an increase in electron flux incident on the innermost molecule from within the metal generates a larger amplitude force in linear measure. (The same assumption is implicit in the discussion of Fig. 11 given above.) This is tantamount to invoking, within one interpretation [1], thermal excitation of low-frequency vibrational modes during the laser pulse such that, as the intensity of the incident light is increased, $\psi(z,Q;t)$ is transferred to $V_0(z;Q)$ at increasingly repulsive parts of the potential (see Fig. 7). A DIMET (desorption induced by multiple electronic transitions) scheme, whereby multiple z transits of the excited-state potential $V_1(z;Q)$ by a transient superposition state results in a greater initial desorptive impulse, would yield a nonlinear dependence of F_0 on the laser intensity [9(b),14–16].

For given N and τ_p, calculations of $z(t)$ and $\dot{z}(t)$ are performed for a range of values of $F(x,y;t)$ along a line radiating outwards from the central laser spot where $F(x,y;t)=F_0$ to the limit where $F(x,y;t)=F_0/40$, discretized as described above; every direction is assumed to be the same, given the form of Eq. (9), and we integrate over the number of hexagonal tubes enclosed within the disc illuminated by the laser profile. From this information, the fraction $f(v_z)$ of the total number of irradiated molecules with desorption velocities in the range $v_z \rightarrow v_z + dv_z$ is computed. The size of each velocity bin, dv_z, is typically 10 or 1 ms^{-1} as stated in the captions to Figs. 12–14; for large driving forces, though, a value of $dv_z = 100$ ms^{-1} was selected on grounds of computational convenience. By way of comparison, in the experiments of Ref. [1], a TOF resolution of ± 1 μs measured over the flight path between metal surface and mass spectrometer rendered a precision in velocity measurements of approximately ± 20 ms^{-1} at $v_z = 2000$ ms^{-1} and ± 0.05 ms^{-1} at $v_z = 100$ ms^{-1}.

Figures 12–14 present results in the form of bar graphs of $f(v_z)$ at different values of the desorption velocity $v_z = \dot{z}(t)$. Figure 12 shows how the distribution varies as a function of the number of layers N for given τ_P and F_0. It can be seen that: for $N>2$, the innermost layer that desorbs in the forward direction [that is, without rebounding towards the metal surface, $n=5$, 8, and 17 for Figs. 12(b), (c), and (d), respectively], results in a narrow distribution of low velocities with $v_z \leqslant 700$ ms^{-1}, the width of which is maximal for $N \simeq 10$; layers further removed from the source of the initial impact result in broader distributions of $f(v_z)$ that extend up to $v_z \simeq 3400$–5000 ms^{-1} for the particular combination of τ_P and F_0 investigated here; for each value of N, the outermost layer results in the broadest distribution, with line dissociation over the entire range of permissible velocities from $v_z \simeq 200$ ms^{-1} $(N=7$, 10, and 20) up to $v_z > 10\,000$ ms^{-1} $(N=2)$; the highest dissociation velocity attained by the outermost particle is smallest for the largest number of intervening molecular layers and vice versa. There are therefore three or four distinct distributions $f(v_z)$ at all N, depending on the number of desorbing layers, except for $N=2$, in which case there is obviously only one, broad $f(v_z)$. For $N>2$, the general pattern of a narrow $f(v_z)$ peaked at low velocities with a series of broader distributions extending to higher v_z is found for all $N \leqslant 20$ investigated in this study. More so than with Figs. 9–11, these calculations can be compared directly with the experimental results plotted in Fig. 1 of Ref. [1(a)] and Fig. 2 of Ref. [1(b)], which display TOF spectra for photoejection of Bz from Pt induced by 150-fs laser pulses at different molecular coverages (i.e., N). Such a comparison shows that the calculated values of $f(v_z)$ extend to much higher velocities than observed in the laboratory by a factor of approximately 2, indicating that the model of resonant electron scattering supplies a value of $F(\epsilon;\tau_R)$ that is too large. However, the results of Fig. 12 are in qualitative agreement with experiment in that they predict liftoff of intact molecules from the metal surface with different characteristic velocity distributions and how they vary with N. The different shapes of the calculated and experimental distributions is discussed below.

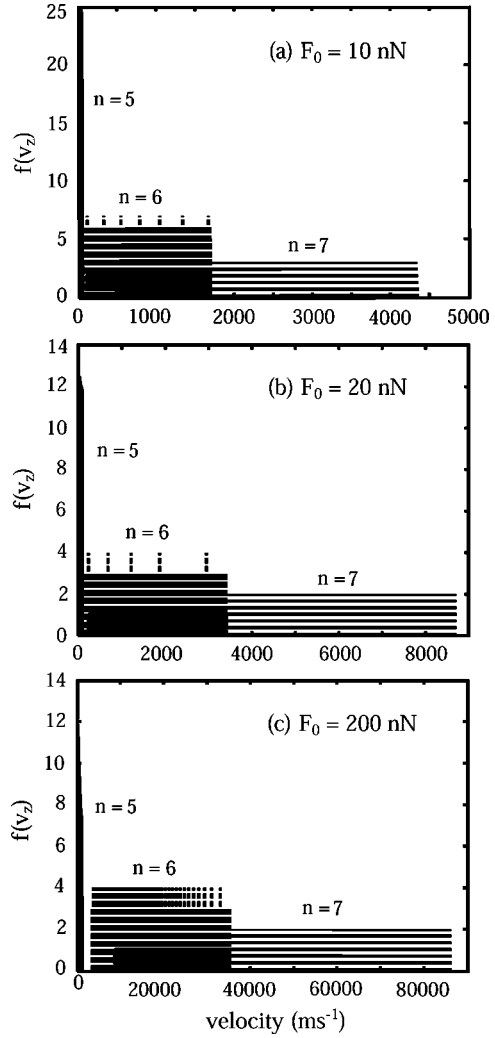

FIG. 13. Bar charts showing the fraction $f(v_z)$ of molecules with desorption velocities v_z as a function of v_z for $N=7$ layers subject to different maximum driving forces of $F_0=10$ (a), 20 (b), and 200 (c) nN. $F(t)$ has a constant Gaussian FWHM of $\tau_P=100$ fs. Panel (a) displays $10^2 f(v_z)$ $(n=5)$ and $10^3 f(v_z)$ $(n=6$ and 7); panel (b) displays $f(v_z)$ for all n; panel (c) displays $10^2 f(v_z)$ $(n=5)$ and $10^3 f(v_z)$ $(n=6$ and 7). Bin sizes dv_z are 10 ms^{-1} for panels (a) and (b) and 100 ms^{-1} for panel (c).

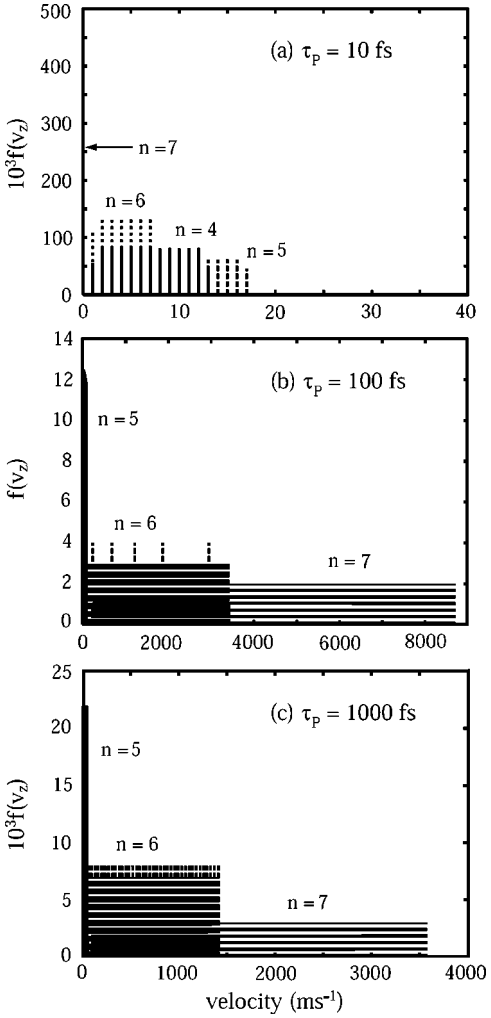

FIG. 14. Bar charts showing the fraction $f(v_z)$ of molecules with desorption velocities v_z as a function of v_z for $N=7$ layers subject to terminal Gaussian temporal impacts of varying FWHM $\tau_P=10$ (a), 100 (b), and 1000 (c) fs. $F(t)$ has a constant maximum amplitude of $F_0=20$ nN. Panels (a) and (c) display $10^3 f(v_z)$ for all n; panel (b) displays $10^2 f(v_z)$ $(n=5)$ and $10^3 f(v_z)$ $(n=6$ and 7). Bin sizes dv_z are 1 ms^{-1} for panel (a) and 10 ms^{-1} for panels (b) and (c).

Figure 13 shows the variation of $f(v_z)$ with terminal impact amplitude for $N=7$ and constant $\tau_P=100$ fs. In this case we see that although the pattern of three distinct $f(v_z)$ distributions is maintained at values of $F_0=10$, 20, and 200 nN, the distribution of desorption velocities of the two outermost layers, labeled $n=6$ and $n=7$, widens substantially as the driving force is increased. Line fragmentation at $n=5$, however, proceeds with a relatively narrow distribution of velocities irresepctive of the magnitude of F_0, and the maximum ejection velocity of the fifth molecular layer increases approximately linearly with F_0 (by a factor of 28 compared to 20).

The distributions obtaining for impulses with an identical maximum amplitude F_0 but different impact durations are portrayed in Fig. 14 for $N=7$. The goal of these calculations is to examine collisional energy transfer when the driving force is shorter than, comparable to and far in excess of the oscillation period ω_0^{-1} of molecules arranged on the metal surface in the absence of an external perturbation: in these model calculations, $\omega_0^{-1}=93$ fs for Bz [29] irrespective of N. There is no mediation of $F(t)$ due to the response of the substrate to the **E** field of the incident laser light. To include the temporal organization of the electron distribution at the metal surface due to photon impact requires calculations of the electron dynamics appropriate to the structure at the molecule-metal interface as well as, if the supposition of Ref. [1(b)] is correct, input from phonon modes of the lattice during irradiation [37]. For $\tau_P=100$ fs, we see that the outermost $n=7$ layer can dissociate from the remainder at velocities in excess of 8500 ms^{-1}, while the penulimate $n=6$ layer is ejected at velocities up to $\simeq 3500$ ms^{-1}. When the pulse width is increased tenfold to $\tau_P=1000$ fs, the de-

sorption velocities of the two outermost layers are substantially reduced, by more than a factor of 0.5, though their distributions are still broad in comparison to $f(v_z)$ for the $n=5$ layer. When τ_P is shortened to 10 fs, a fourth fragmentation channel opens up, the line dissociation velocities are massively reduced, and the pattern of velocity distributions is altered. In this case, by contrast with the results of Figs. 12 and 13, it is the outermost molecular layer which fragments from the line with the lowest velocities, $v_z=1$ and 2 ms^{-1}, and the narrowest distribution of velocities. The penultimate $n=6$ layer also lifts off slowly, but with a broader spread in v_z. The molecules that desorb fastest, and with the broadest distribution of $f(v_z)$, are those that originate from the third outermost layer $n=5$, for which $f(v_z)$ shows values up to $v_z=17$ ms^{-1}; the next inner layer, $n=4$, which emerges with velocities $v_z \leqslant 14$ ms^{-1}, also has a broad distribution in $f(v_z)$ in comparison to those for the two outermost layers.

The results of Fig. 14 stand in qualitative agreement with Figs. 2 and 4 of Ref. [1(b)]. Both calculated and experimental values of $f(v_z)$ shift to a lower range of velocities when the impulse duration is increased such that $\tau_P \gg \omega_0^{-1}$; the experimental $f(v_z)$ distribution also becomes distinctly non-Maxwellian in form (see below). From Fig. 14 it may be concluded that to achieve the highest line fragmentation (desorption) velocities for a given F_0, which is stated to be directly proportional to the maximum incident laser fluence (see earlier), it is necessary to select a pulse width that closely matches the natural oscillation period of the impacted molecules about their equilibrium locations (neglecting anharmonic effects). When $\tau_P=\omega_0^{-1}$, the impacting force achieves its maximum value at the same time at which the innermost molecule, assumed to be positioned initially at its equilibrium coordinate z_{eq} for the purposes of this discussion, returns to the same location with maximum velocity one half cycle later, and is thus able to deliver maximum impact on the neighboring molecule (Fig. 7): since it is assumed that the same value of ω_0 pertains to molecules in different layers and that degradation of collisional energy transfer through orthogonal inelastic effects may be neglected, this choice of τ_P results in molecules in the outermost layer receiving a maximal impact. When $\tau_P \gg \omega_0^{-1}$, the effect of numerous oscillation cycles executed by the molecules during the impacting pulse is to destroy the developing phase relationship (coherence) between the attainment of F_0 by the applied force and the completion of the first half cycle of the molecular oscillation. When $\tau_P \ll \omega_0^{-1}$, the terminal impact is simply not applied for long enough in comparison to $\omega_0^{-1}/2$ for maximal transfer of the initial impact along the line. In both these latter situations, the resultant force experienced by molecules $n \geqslant 2$ is diminished relative to the value of the applied F_0, giving rise to smaller line fragmentation velocities.

What is also clear by inspection of Figs. 12–14 is that the distributions $f(v_z)$ are not Maxwellian. The authors of Ref. [1] fitted measured $f(v_z)$ obtained under conditions of differing light fluence, pulse duration, and molecular layers to a sum of three modified Maxwellian distributions of the form

$$f(v_z)=\sum_{i=1}^{3} a_i v_z^3 \exp[-m(v_z-u_i)^2/2kT_i], \qquad (10)$$

where T_i is the temperature associated with the ith distribution, a_i is its amplitude and u_i the stream velocity. Furlan has recently criticized the isolated use of thermal distribution functions such as Eq. (10) to describe translational energy distributions that are inherently non-Maxwellian [38], noting the need for a model of the impact and subsequent dissociation to accompany the measured energy partioning, as is well established for measurements of translational energy release in gas-phase dissociations [39]. Restrictions on the use of Maxwellian distributions to describe molecular TOF measurements under non-Maxwellian conditions have been discussed elsewhere [38,40] and are not repeated here. A formal analysis [41] of thermally driven desorption from surfaces based on the method of moments, in which particle interactions in the gas phase close to the surface are treated explicitly, leads to the adoption of a Maxwell-Boltzmann distribution characterized by a single temperature for the development velocities of photoejected materials. This result has been utilized in a number of investigations of Knudsen layer formation in laser-induced sputtering and ablation of half a monolayer or less of material in 10-ns pulses [42]. Monte Carlo simulations, on the other hand, suggest the applicabiltity of a two-temperature model [43], though the arguments in support of such an approach are based on curve fitting rather than theory. For ablation of more than 0.5 monolayer and nonthermally driven processes [42], where the Knudsen layer breaks down to form an unsteady adiabatic expansion, it is not entirely obvious that equations such as Eq. (10) can be meaningfully employed.

Functional forms such as Eq. (10) have, however, been invoked to describe laser-induced desorption of range of molecules from metallic and nonmetallic surfaces [43,44], notwithstanding arguments concerning the usefulness and correctness of such an approach. What is clear from Figs. 12–14 is that, within the remit of the model described in this section, an impulsive impact on a molecule adjacent to a metal surface followed by classical energy transfer across the adsorbed layers does not inherently lead to molecules ejected into the gas phase with kinetic energies distributed according to a Maxwellian expectation. This in itself is not surprising: the initial electron-induced impact assumed here is not of thermal origin and and there are no subsequent thermalizing collisions as energy is transferred to the outermost particles.

V. SHORTCOMINGS OF THE MODEL CALCULATIONS

It is appreciated that there are many. In particular, it is possible to identify four central features of the scheme presented in Sec. IV as applied to ultrafast laser desorption of molecular layers that could be improved upon in more sophisticated calculations:

(i) Application of the model to impulsive molecular desorption is predicated upon ultrafast, coherent electron-hole scattering as the origin of the initial force that is directed along the surface normal, away from the metal. Of paramount importance to a complete description of the effect of light on transparent molecules attached to a low-temperature

solid is the connection between the time development of the incident photon field and that of the impulsive force that triggers the initial impact on molecules closest to the metal surface. An analysis of the substrate temporal response that intervenes in time between the effect of the laser pulse and the onset of collisional energy transfer is needed to specify the transient hot electron distribution generated during the light pulse. For unidirectional thermionic electron emission, Gadzuk has carried out the pertinent calculations of the growth and decay of a thermal electron flux at a metal surface as a function of different desorption energies [16]. The relation between the time dependences of a photon-generated electron flux, the electrical forces it sets up at the surface and the incoming light beam is what is required in a more elaborate theoretical description than that presented here.

For the case of Bz attached to Pt{111}, the coupling of a hot electron flux to phonon motions, and how the two cooperate to propel molecules away from the surface, also needs to be understood if the near-linear dependences of Bz desorption yield and translational energy on the incident light intensity is to be recovered in line with recommendations based on the experimental observations [1]. The notion that has been put forward [1(b)] is that electron-phonon excitation of the molecule-surface mode at early times on the leading edge of the laser pulse leads to vibrational pre-heating of the innermost molecule followed by an electron-driven impact and sequential energy transfer across the molecular layers. A vibrationally assisted origin to the impulse directed along the desorption coordinate has not been explicitly included in this work, demanding as it does a consideration of the metal-molecule coupling in a multidimensional space of the relevant vibrational degrees of freedom.

(ii) Information on the packing arrangement of molecules at the surface and in subsequent layers, such as is increasingly available from density functional theory calculations, would be crucial for a detailed study of the effect of the distribution of photon impacts delivered by an incident laser beam with a known spatial intensity profile in both transverse and longitudinal dimensions.

(iii) The interaction between neighboring molecules is assumed to be governed by a Morse potential. For calculations that incorporate the coupling between the field and electrons in terms of the system eigenstates, or a superposition thereof, knowledge of the lowest-lying excited-state potential of the molecule-surface complex is also required.

(iv) No account has been taken of the gas-phase dynamics subsequent to photoejection of molecules from the metal surface. Clustering to form conglomerates has been discussed as a distinct possibility under the prevailing experimental conditions [1].

VI. CONCLUSIONS

This paper discusses the classical dynamics of a line of particles subject to an impulsive driving force at one end: individual particle trajectories leading to the breakup of the line have been computed for different magnitude and duration impulses, and for varying numbers of particles. It is found that multiple fragmentation patterns can be induced, leading to different line dissociation behavior: particles at the end of the line opposite to which the impulse is applied lift off with approximately the initial impact velocity, in accordance with the findings of an earlier investigation [2]; particles that were initially stationed in the middle portion of the line dissociate at slower speeds.

A line of touching spheres has been applied as a model for ultrafast laser irradiation of transparent molecules on a cold metal surface, and leads to qualitatively correct predictions of the desorption behavior as a function of the number of molecular layers attached to the surface and the duration and amplitude of the driving force, the latter determined by laser pulses of varying fluence. From Figs. 9–14, the following deductions may be made, within the context of energy transfer across ''Newton's cradle,'' concerning the desorption of Bz $N>2$ from Pt{111} subject to impacts approximately equal to or longer than the intermolecular oscillation period:

(i) The appearance of a hyperthermal desorption peak in the observed TOF spectrum [1] originates from desorption of the outermost benzene molecules for $N \geqslant 3$, and is independent of the number of intervening layers, at least for $3 \leqslant N \leqslant 20$.

(ii) Slower desorption of molecules initially stationed at intermediate line positions, resulting in observed thermal and subthermal features in the TOF spectrum [1], is favored at large driving impacts, associated with high laser fluences, and for thicker coverages of the metal.

(iii) The distribution of desorption velocities depends on the particular combination of F_0 and τ_P that characterize the initial impact, as well as the number of layers, in a way that is not always *a priori* obvious; i.e., it is not always the case that hyperthermally desorbed molecules originiate from the outermost layer, thermal molecules from intermediate portions of the line, and molecules with the slowest, subthermal velocities from locations closest to the source of the initial impact.

(iv) The yield of hyperthermally desorbed molecules increases with coverage for thicknesses corresponding to $3 \leqslant N \leqslant 20$.

These deductions are independent of the exact origin of the force that drives the initial impact at a metal surface and how it is modified by the dynamical response of the solid to laser light. They are also in agreement with the conclusions stated in the papers of Arnolds *et al.* [1], and lend support to the postulated mechanism of rapid energy transfer between adsorbed molecular layers. Because of the approximations that are invoked to model multilayer molecular desorption from metals, it is not possible to comment on the usefulness of measured TOF distributions as a quantitatively sensitive probe of the molecule-molecule and molecule-surface interactions. Predictions of the model and experimental results could be brought into closer agreement with an substantially improved treatment of the light-matter interaction Hamiltonian and intermolecular potentials. These and other shortcomings of this approach have been discussed.

ACKNOWLEDGMENT

The author acknowledges the Royal Society of London for funds to purchase a workstation.

[1] (a) H. Arnolds, C. E. M. Rehbein, G. Roberts, R. J. Levis, and D. A. King, Chem. Phys. Lett. **314**, 389 (1999); (b) J. Phys. Chem. **104**, 3375 (2000).

[2] E. J. Hinch and S. Saint-Jean, Proc. R. Soc. London, Ser. A **455**, 3201 (1999).

[3] V. F. Nesterenko, J. Appl. Mech. Tech. Phys. **5**, 733 (1983).

[4] C. Coste, E. Falcon, and S. Fauve, Phys. Rev. E **56**, 6104 (1997).

[5] J. B. Marion and S. T. Thornton, *Classical Dynamics of Particles and Systems*, 3rd ed. (Harcourt Brace Jovanovich Inc., Orlando, 1988), Chap. 3, pp. 128–135.

[6] W. H. Press, B. P. Flannery, S. A. Teukolsky, and W. T. Vetterling, *Numerical Recipes* (Cambridge University Press, Cambridge, England, 1987), Chap. 15, pp. 550–560.

[7] L. V. Zhigilei and B. J. Garrison, J. Appl. Phys. **88**, 1281 (2000); Appl. Phys. Lett. **74**, 1341 (1999); P. B. S. Kodali, L. V. Zhigilei, and B. J. Garrison, Nucl. Instrum. Methods Phys. Res. B **153**, 167 (1999); R. Zoric, B. Pearson, K. D. Krantzman, and B. J. Garrison, Int. J. Mass Spectrom. Ion Processes **174**, 155 (1998); L. V. Zhigilei, P. B. S. Kodali, and B. J. Garrison, J. Phys. Chem. B **102**, 2845 (1998), and references therein.

[8] In Fig. 1, results for a linear and 3/2-power-law dependence on interparticle separation are shown, because these dependences derive from Hertz contact theory for the interaction between spherical shells and solid spheres, respectively (more details are given in Ref. [2]).

[9] (a) J. W. Gadzuk, in *Femtosecond Chemistry*, edited by J. Manz and L. Wöste (VCH, Weinheim, 1995), Vol. 2, Chap. 20, pp. 603–624, and references therein; (b) J. Phys. B **31**, 4061 (1998); (c) J. Electron Spectrosc. Relat. Phenom. **99**, 321 (1999).

[10] E. Knoesel, T. Hertel, M. Wolf, and G. Ertl, Chem. Phys. Lett. **240**, 409 (1995); M. Bauer, S. Pawlik, and M. Aeschlimann, Phys. Rev. B **55**, 10 040 (1997); A. Hotzel, K. Ishioka, E. Knoesel, M. Wolf, and G. Ertl, Chem. Phys. Lett. **285**, 271 (1998); L. Bartels, G. Meyer, K. H. Rieder, D. Velic, E. Knoesel, A. Hotzel, M. Wolf, and G. Ertl, Phys. Rev. Lett. **80**, 2004 (1998); K. Ishioka, C. Gahl, and M. Wolf, Surf. Sci. **454**, 73 (2000); C. Gahl, K. Ishioka, Q. Zhong, A. Hotzel, and M. Wolf, Faraday Discuss. **117**, 191 (2000).

[11] S. Ogawa, H. Nagano, and H. Petek, Appl. Phys. B: Lasers Opt. **68**, 611 (1999); Phys. Rev. Lett. **82**, 1931 (1999); Surf. Sci. **428**, 34 (1999); H. Petek, M. J. Weida, H. Nagano, and S. Ogawa, *ibid.* **451**, 22 (2000).

[12] R. Franchy, F. Bartolucci, F. B. de Mongeot, F. Cemic, M. Rocca, U. Valbusa, L. Vattuone, S. Lacombe, K. Jacobi, K. B. K. Tang, R. E. Palmer, J. Villette, D. Teillet-Billy, and J. P. Gauyacq, J. Phys. C **12**, R53 (2000); J. P. Gauyacq, A. G. Borisov, G. Raseev, and A. K. Kazansky, Faraday Discuss. **117**, 15 (2000).

[13] See, for example, Z. W. Gortel, R. Teshima, and H. J. Kreuzer, Phys. Rev. B **37**, 3183 (1988); J. W. Gadzuk and C. W. Clark, J. Chem. Phys. **91**, 3174 (1989); Z. W. Gortel and A. Wierzbicki, Phys. Rev. B **43**, 7487 (1991); J. W. Gadzuk, J. Electron Spectrosc. Relat. Phenom. **54**, 201 (1990); H. Guo, Chem. Phys. Lett. **240**, 393 (1995); P. Saalfrank, S. Holloway, and G. R. Darling, J. Chem. Phys. **103**, 6720 (1995); H. Guo and T. Seideman, *ibid.* **103**, 9062 (1995); L. Liu, H. Guo, and T. Seideman, *ibid.* **104**, 8757 (1996); H. Guo, *ibid.* **106**, 1967 (1997); R. Franchy, Rep. Prog. Phys. **61**, 691 (1998).

[14] See, for example, P. Saalfrank, R. Baer, and R. Kosloff, Chem. Phys. Lett. **230**, 463 (1994); P. Saalfrank, Chem. Phys. **193**, 119 (1995); **211**, 265 (1996); P. Saalfrank, R. Baer, and R. Kosloff, J. Chem. Phys. **105**, 2441 (1996); H. Guo and L. Liu, Surf. Sci. **372**, 337 (1997); T. Seideman, J. Chem. Phys. **106**, 417 (1997); T. Seideman and H. Guo, *ibid.* **107**, 8627 (1997); H. Guo, P. Saalfrank, and T. Seideman, Prog. Surf. Sci. **62**, 239 (1999).

[15] T. F. Heinz, J. A. Misewich, and D. M. Newns, Prog. Theor. Phys. Suppl. **106**, 411 (1991); J. A. Misewich, T. F. Heinz, and D. M. Newns, Phys. Rev. Lett. **68**, 3737 (1992); N. Chakrabati, N. Sathyamurthy, and J. W. Gadzuk, J. Phys. Chem. A **102**, 4154 (1998).

[16] J. W. Gadzuk, Chem. Phys. **251**, 87 (2000).

[17] E. G. d'Agliano, P. Kumar, W. Schaich, and H. Suhl, Phys. Rev. B **11**, 2122 (1975); C. Springer, M. Head-Gordon, and J. C. Tully, Surf. Sci. **320**, L57 (1994); M. Brandbyge, P. Hedegård, T. F. Heinz, J. A. Misewich, and D. M. Newns, Phys. Rev. B **52**, 6042 (1995); M. Head-Gordon and J. C. Tully, J. Chem. Phys. **103**, 10 137 (1995); C. Springer and M. Head-Gordon, Chem. Phys. **205**, 73 (1996); J. T. Kindt, J. C. Tully, M. Head-Gordon, and M. A. Gomez, J. Chem. Phys. **109**, 3629 (1998).

[18] J. A. Prybyla, T. F. Heinz, J. A. Misewich, M. M. T. Loy, and J. H. Glownia, Phys. Rev. Lett. **64**, 1537 (1990); F. Budde, T. F. Heinz, M. M. T. Loy, J. A. Misewich, F. de Rougemont, and H. Zacharias, *ibid.* **66**, 3024 (1991); F. Budde, T. F. Heinz, A. Kalamarides, M. M. T. Loy, and J. A. Misewich, Surf. Sci. **283**, 143 (1993).

[19] J. A. Prybyla, H. W. K. Tom, and G. D. Aumiller, Phys. Rev. Lett. **68**, 503 (1992); F.-J. Kao, D. G. Busch, D. Gomes da Costa, and W. Ho, *ibid.* **70**, 4098 (1993); F.-J. Kao, D. G. Busch, D. Cohen, D. Gomes da Costa, and W. Ho, *ibid.* **71**, 2094 (1993); J. A. Misewich, A. Kalamarides, T. F. Heinz, U. Höfer, and M. M. T. Loy, J. Chem. Phys. **100**, 736 (1994); D. G. Busch, S. Gao, R. A. Pelak, M. F. Booth, and W. Ho, Phys. Rev. Lett. **75**, 673 (1995); D. G. Busch and W. Ho, *ibid.* **77**, 1338 (1996).

[20] R. W. Schoenlein, J. G. Fujimoto, G. L. Eesley, and T. W. Capehart, Phys. Rev. Lett. **61**, 2596 (1988); Phys. Rev. B **41**, 5436 (1990); **43**, 4688 (1991); R .L. Lingle, Jr., N.-H. Ge, R. E. Jordan, J. D. McNeill, and C. B. Harris, Chem. Phys. **205**, 191 (1996); M. Wolf, E. Knoesel, and T. Hertel, Phys. Rev. B **54**, R5295 (1996); T. Hertel, E. Knoesel, M. Wolf, and G. Ertl, Phys. Rev. Lett. **76**, 535 (1996); J. D. McNeill, R. L. Lingle, Jr., N.-H. Ge, C. M. Wong, R. E. Jordan, and C. B. Harris, *ibid.* **79**, 4645 (1997); T. Hertel, E. Knoesel, A. Hotzel, M. Wolf, and G. Ertl, J. Vac. Sci. Technol. A **15**, 1503 (1997); M. Wolf, Surf. Sci. **377-379**, 343 (1997); U. Höfer, I. L. Shumay, Ch. Reuβ, U. Thomann, W. Wallauer, and Th. Fauster, Science **207**, 1480 (1997); N.-H. Ge, C. M. Wong, R. L. Lingle, Jr., J. D. McNeill, K. J. Gaffney, and C. B. Harris, *ibid.* **279**, 202 (1998); E. Knoesel, A. Hotzel, and M. Wolf, J. Electron Spectrosc. Relat. Phenom. **88**, 577 (1998); A. Hotzel, C. Moos, K. Ishioka, M. Wolf, and G. Ertl, Appl. Phys. B: Lasers Opt. **68**, 615 (1999); K. Ishioka, C. Gahl, and M. Wolf, Surf. Sci. **454**, 73 (2000); K. J. Gaffney, S. H. Liu, A. D. Miller, P. Szyman-

ski, and C. B. Harris, J. Chin. Chem. Soc. (Taipei) **47**, 759 (2000).
[21] (a) K. J. Gaffney, C. M. Wong, S. H. Liu, A. D. Miller, J. D. McNeill, and C. B. Harris, Chem. Phys. **251**, 99 (2000); (b) D. Velic, A. Hotzel, M. Wolf, and G. Ertl, J. Chem. Phys. **109**, 9155 (1998).
[22] E. Knoesel, A. Hotzel, T. Hertel, M. Wolf, and G. Ertl, Surf. Sci. **368**, 76 (1996); E. Knoesel, A. Hotzel, and M. Wolf, Phys. Rev. B **57**, 12 812 (1998); M. Wolf, A. Hotzel, E. Knoesel, and D. Velic, *ibid.* **59**, 5926 (1999); M. Bonn, D. N. Denzler, S. Funk, M. Wolf, S. S. Wellershof, and J. Hohlfeld, *ibid.* **61**, 1101 (2000); A. Hotzel, M. Wolf, and J. P. Gauyacq, J. Phys. Chem. B **104**, 8455 (2000).
[23] H. Petek and S. Ogawa, Prog. Surf. Sci. **56**, 239 (1997), and references therein; T. Sjodin, H. Petek, and H.-L. Dai, Phys. Rev. Lett. **81**, 5664 (1998); H. Petek, H. Nagano, and S. Ogawa, Appl. Phys. B: Lasers Opt. **68**, 369 (1999); Phys. Rev. Lett. **83**, 832 (1999); A. G. Borisov, A. K. Kazansky, and J. P. Gauyacq, Surf. Sci. **430**, 165 (1999); B. Grumhalter and H. Petek, *ibid.* **445**, 195 (2000); H. Petek, H. Nagano, M. J. Weida, and S. Ogawa, Chem. Phys. **251**, 71 (2000); T. Sjodin, C.-M. Li, H. Petek, and H.-L. Dai, *ibid.* **251**, 205 (2000); A. G. Borisov, J. P. Gauyacq, A. K. Kazansky, E. V. Chulkov, V. M. Silkin, and P. M. Echenique, Phys. Rev. Lett. **86**, 488 (2001).
[24] (a) J. W. Gadzuk, Surf. Sci. **342**, 345 (1995); (b) Phys. Rev. Lett. **76**, 4234 (1996).
[25] A. Herzenberg and E. Stryjewski, Phys. Rev. A **15**, 234 (1977); J. P. Gauyacq, J. Chem. Phys. **93**, 384 (1990).
[26] (a) J. W. Gadzuk, L. J. Richter, S. A. Buntin, D. S. King, and R. R. Cavanagh, Surf. Sci. **235**, 317 (1990); (b) J. W. Gadzuk, Phys. Rev. B **44**, 13 466 (1991).
[27] P. R. Antoniewicz, Phys. Rev. B **21**, 3811 (1980).
[28] Ph. Avouris, P. S. Bagus, and A. R. Rossi, J. Vac. Sci. Technol. B **3**, 1484 (1985); Ph. Avouris, P. S. Bagus, and C. J. Nelin, J. Electron Spectrosc. Relat. Phenom. **38**, 269 (1986); J. W. Gadzuk, in *Laser Spectroscopy and Photochemistry on Metal Surfaces*, edited by H.-L. Dai and W. Ho (World Scientific, Singapore, 1995), p. 897.
[29] C. M. Mate and G. A. Somorjai, Surf. Sci. **160**, 542 (1985).
[30] P. Jakob and D. Menzel, Surf. Sci. **220**, 70 (1989).
[31] (a) J. L. Gland and G. A. Somorjai, Surf. Sci. **38**, 157 (1973); (b) P. C. Stair and G. A. Somorjai, J. Chem. Phys. **67**, 4361 (1977).
[32] S. Lehwald, H. Ibach, and J. E. Demuth, Surf. Sci. **78**, 577 (1978).
[33] P. Jakob and D. Menzel, J. Chem. Phys. **105**, 3838 (1996).
[34] I am grateful to Dr. H. Arnolds for her advice on this value.
[35] R. Chaterjee, Z. Postawa, N. Winograd, and B. J. Garrison, J. Phys. Chem. B **103**, 151 (1999); Ref. [41] of this paper.
[36] H. J. Korsch, A. Ernesti, and J. A. Núñez, J. Phys. B **25**, 773 (1992).
[37] C. Thomsen, H. T. Grahn, H. J. Maris, and J. Tauc, Phys. Rev. B **34**, 4129 (1986).
[38] A. Furlan, Chem. Phys. Lett. **321**, 339 (2000).
[39] See, for example, R. D. Levine and R. B. Bernstein, in *Dynamics of Molecular Collisions*, edited by W. H. Miller (Plenum Press, New York, 1976), Chap. 7, pp. 336–352; J. C. Lorquet, J. Phys. Chem. A **104**, 5422 (2000).
[40] L. V. Zhigilei and B. J. Garrison, Appl. Phys. Lett. **71**, 551 (1997); X.-Y. Zhu, Annu. Rev. Phys. Chem. **45**, 113 (1994).
[41] C. Cerignani, in *Rarefied Gas Dynamics*, edited by S. S. Fisher (AIAA, New York, 1981), p. 305.
[42] H. M. Urbassek and J. Michl, Nucl. Instrum. Methods Phys. Res. B **22**, 480 (1987); R. Kelly, J. Chem. Phys. **92**, 5047 (1990); B. Braren, K. G. Casey, and R. Kelly, Nucl. Instrum. Methods Phys. Res. B **58**, 463 (1991).
[43] I. NoorBatcha, R. R. Lucchese, and Y. Zeiri, Surf. Sci. **200**, 113 (1988); J. Chem. Phys. **89**, 5251 (1988).
[44] R. Braun and P. Hess, J. Chem. Phys. **99**, 8330 (1993); J. E. Fieberg, G. J. Szulczewski, and J. M. White, Chem. Phys. Lett. **290**, 268 (1998); J. E. Fieberg and J. M. White, *ibid.* **306**, 103 (1999).